Sulforaphane alleviates lung ischemia-reperfusion injury through activating Nrf-2/HO-1 signaling

LIANG ZHANG[1], SHUXIAN WANG[2], YING ZHANG[3], FENGHUAN LI[1], and CHAOXIAO YU[1]

[1]Department of Respiratory and Critical Care Medicine, Yantaishan Hospital, Yantai, Shandong 264001; [2]Department of Respiratory, Yantai Beihai Hospital, Yantai, Shandong 265701; [3]Department of Emergency, Tai'an Central Hospital, Tai'an, Shandong 271000, P.R. China

Received August 22, 2022; Accepted March 10, 2023

DOI: 10.3892/etm.2023.11964

Abstract. Oxidative stress and inflammation are both involved in the pathogenesis of lung ischemia-reperfusion (I/R) injury. Sulforaphane (SFN) is a natural product with cytoprotective, anti-inflammatory, and antioxidant properties. The present study hypothesized that SFN may protect against lung I/R injury via the regulation of antioxidant and anti-inflammatory-related pathways. A rat model of lung I/R injury was established, and rats were randomly divided into 3 groups: Sham group, I/R group, and SFN group. It was shown that SFN protected against a pathological inflammatory response via inhibition of neutrophil accumulation and in the reduction of the serum levels of the pro-inflammatory cytokines, IL-6, IL-1β, and TNF-α. SFN treatment also significantly inhibited lung reactive oxygen species production, decreased the levels of 8-OH-dG and malondialdehyde, and reversed the decrease in the antioxidant activities of the enzymes catalase, superoxide dismutase, and glutathione peroxidase in the lungs of the I/R treated rats. In addition, SFN ameliorated I/R-induced lung apoptosis in rats by suppressing Bax and cleaved caspase-3 levels and increased Bcl-2 expression. Furthermore, SFN treatment activated an Nrf2-related antioxidant pathway, as indicated by the increased nuclear transfer of Nrf2 and the downstream HO-1 and NADPH quinone oxidoreductase-1. In conclusion, these findings suggested that SFN protected against I/R-induced lung lesions in rats via activation of the Nrf2/HO-1 pathway and the accompanied anti-inflammatory and anti-apoptotic effects.

Introduction

Lung ischemia-reperfusion (I/R) injury is a common complication that occurs following lung transplantation, cardiopulmonary bypass, pulmonary embolism thrombectomy, and other surgical procedures (1,2). Despite improvements in medical procedures, the incidence of lung I/R injury remains high as has the clinical mortality rate following, especially in lung transplantation (3).

During the lung I/R process, excessive levels of inflammatory mediators and reactive oxygen species (ROS) are released into the circulation, with a crucial role in the sequence of events leading to lung failure (4). Indeed, both inflammatory response and oxidative stress have been found to contribute to the pathogenesis of multi-lung injuries and the inhibition of inflammation and oxidative stress was shown to ameliorate lung injuries (5-7).

Sulforaphane (SFN) is an isothiocyanate derived by the hydrolysis of glucosinolates via the enzyme myrosinase and is enriched in cruciferous vegetables, particularly in broccoli sprouts (8). SFN plays a vital role in redox homeostasis, exerting a cytoprotective action against oxidative stress via activation of Nrf2-related pathways (9-11). Recent studies have shown that the beneficial effects of SFN in I/R-related diseases are due to its antioxidant and anti-inflammatory properties (12). For example, SFN could protect against I/R injury in the liver by activating the Nrf2/ARE pathway (13). Furthermore, the cardioprotective effects of SFN against oxidative stress in cardiomyocytes undergoing I/R were mediated by activation of the Nrf2/HO-1 pathway (14).

Oxidative stress and inflammatory responses underlie several pathological conditions, including I/R injury, and metabolic and age-related diseases. Natural compounds such as SFN may trigger a cellular self-defense mechanism that can effectively mitigate oxidative stress commonly associated with several diseases (15). During the lung I/R process, excessive levels of inflammatory mediators and ROS are released into the circulation, ultimately leading to lung failure; however, the molecular mechanism of SFN on lung I/R injury remains unclear. Therefore, here, the hypothesis that SFN may protect the lung against I/R-induced oxidative stress and inflammation via regulation of the Nrf2-related antioxidant pathway was assessed, based on the following evidence: i) Lung I/R injury is closely associated with oxidative stress and inflammation (6,16); ii) oxidative stress and subsequent apoptosis are involved in lung function disorder (17); iii) SFN was shown to exert a protective effect against oxidative stress via the Nrf2-related antioxidant pathway (18).

Correspondence to: Dr Chaoxiao Yu, Department of Respiratory and Critical Care Medicine, Yantaishan Hospital, 10,087 Keji Road, Laishan, Yantai, Shandong 264001, P.R. China
E-mail: yuchaoxiao@bzmc.edu.cn

Key words: Sulforaphane, lung, ischemia-reperfusion injury, Nrf-2/HO-1, reactive oxygen species

The present study aimed to explore the effects of SFN against lung I/R-induced inflammation and oxidative stress and the potential mechanisms involved.

Materials and methods

Animal management and ethical statement. Male Wistar rats (200-250 g) aged 8-9 weeks were obtained from the animal research center at Lvye Pharmaceutical Co., Ltd. in Shandong, China (certificate number SYXK 2018-0028). Rats were housed in a standard environment with a regular light/dark cycle and free access to water and standard chow. The project was approved by the Ethics Committee of Yantai Mountain Hospital, Yantai, China (approval no. 2021-12.). The rats received humane care and all efforts were made to alleviate suffering.

Establishment of the lung I/R model. The rat model of lung I/R injury was induced as described previously (19). Pentobarbital sodium (50 mg/kg, i.p.) was used to fully anesthetize rats, which were then placed on a homeothermic table to maintain the core body temperature at 37˚C. The left pulmonary hilum was clamped with a noninvasive arterial clip, resulting in complete ischemia and hypoxia of the left lung for 1 h. Next, the vascular clamp was released for 2 h to restore ventilation and perfusion to the left lung. The rats were anesthetized with ether and sacrificed by exsanguination at the end of the experiment. Death was confirmed by a lack of autonomous respiration, no reflexive responses, and a lack of a heartbeat.

SFN was obtained from MilliporeSigma (cat. no. S4441), and a stock solution of 5 mM was prepared in DMSO (cat. no. #D2650, MilliporeSigma; final concentration <0.1%). Stock solutions were stored at -25˚C. The stock solution was diluted using 0.9% NaCl solution into 30 mg/kg as previously reported (20). The rats were divided into three equal and random groups (n=10): Sham group, rats subjected to the same thoracotomy procedure but without a hilar block; SFN group, rats subjected to lung I/R injury given SFN (30 mg/kg/day) by intraperitoneal injection for 7 consecutive days before the I/R model was established; I/R group, rats subjected to lung I/R injury were given the same volume of 0.9% NaCl solution. Fig. 1B shows a schematic diagram of the grouping and interventions.

Blood samples were taken from the femoral artery after reperfusion. Subsequently, the animals were sacrificed with an intravenous overdose of pentobarbital sodium (100 mg/kg). The left lungs were removed for further examination.

Hematoxylin-eosin staining. The middle of the left lung was immediately fixed in 10% formalin and maintained at 4˚C for 24 h. Tissues were dehydrated after 24 h, embedded in paraffin, sectioned at 6 μm, and stained with hematoxylin and eosin for 30 min at room temperature. All images were taken using a Nikon Eclipse 80i microscope (magnification, x400; Nikon Corporation). The extent of lung damage was evaluated blindly using a histological scoring system as described previously (21).

Blood gas analysis. Arterial blood samples were obtained for blood gas analysis. A blood gas analyzer was used to record pH, the partial pressure of oxygen (PaO_2), and the partial pressure of carbon dioxide ($PaCO_2$) in a 0.5 ml sample of arterial blood drawn from the abdominal aorta (RapidPoint 500, Siemens AG).

Detection of lung tissue wet-to-dry (W/D) weight ratio. Wet weight was determined by immediately weighing freshly harvested left upper lung lobe samples. The lung tissue sample was then dried until its weight remained constant. Finally, the dry weight of the lung tissue sample was determined. The lung tissue's W/D weight ratio was calculated by dividing the wet weight by the dry weight.

Detection of pulmonary permeability index. The pulmonary permeability index (PPI) was measured as previously reported (22). To determine total plasma protein, plasma supernatants were obtained and stored at -70˚C. Bronchoalveolar lavage of the lung was performed with 1 ml normal saline. The bronchoalveolar lavage fluid (BALF) was centrifuged at 3,000 x g at 4˚C for 15 min. The BALF supernatant was then stored at -70˚C for the Bradford assay to detect total BALF protein concentration. PPI was calculated by dividing the protein concentration in the BALF by the protein concentration in the plasma.

Detection of myeloperoxidase activity. A total of 100 mg lung tissue was mixed with 1 ml RIPA lysate, homogenized with a glass homogenizer, placed on ice for 30 min to fully lyse the cells, and then centrifuged at 13,000 x g at 4˚C for 15 mi to collect supernatants. The lung tissue myeloperoxidase (MPO) activity was measured using a colorimetry assay kit (cat. no. #A044-1-1, Nanjing Jiancheng Bioengineering Institute) according to the manufacturer's protocol.

Detection of antioxidant capacity. The lung tissues were homogenized and centrifuged to obtain the supernatant as above for the following experimental detections. The activities of glutathione peroxidase (GSH-Px; cat. no. #A005-1-2), superoxide dismutase (SOD; cat. no. A001-3-2), and catalase (CAT; cat. no. #A007-1-1) in lung tissues were assessed by colorimetry using commercial kits (all from Nanjing Jiancheng Bioengineering Institute) as described previously (23).

Detection of oxidative stress. The lung tissues were homogenized and centrifuged to obtain the supernatant for the following experimental detections. ELISA was used to detect 8-OH-dG (cat. no. ab285254; Abcam Co.US) in lung tissues as described previously (24). Briefly, 40 μl sample dilution buffer was added to 10 μl samples in sample wells. A well was left empty as blank control. 8-OH-dG Biotinylated Detection antibody (50 μl; 1:100) was added to each well and incubated for 45 min at 37˚C. The plate sealer was removed and the wells aspirated and refilled with the wash solution. The washing procedure was repeated three times and the plates dried on absorbent filter papers. SABC working solution (100 μl) was added to each well, the plate covered and incubated at 37˚C for 30 min. Then, the solution was discarded and the plate washed five times with 1X Wash Solution. TMB substrate (90 μl) was added to each well and incubated at 37˚C in dark for 15-30 min. The shades of blue should be seen in the first 3-4 wells by the

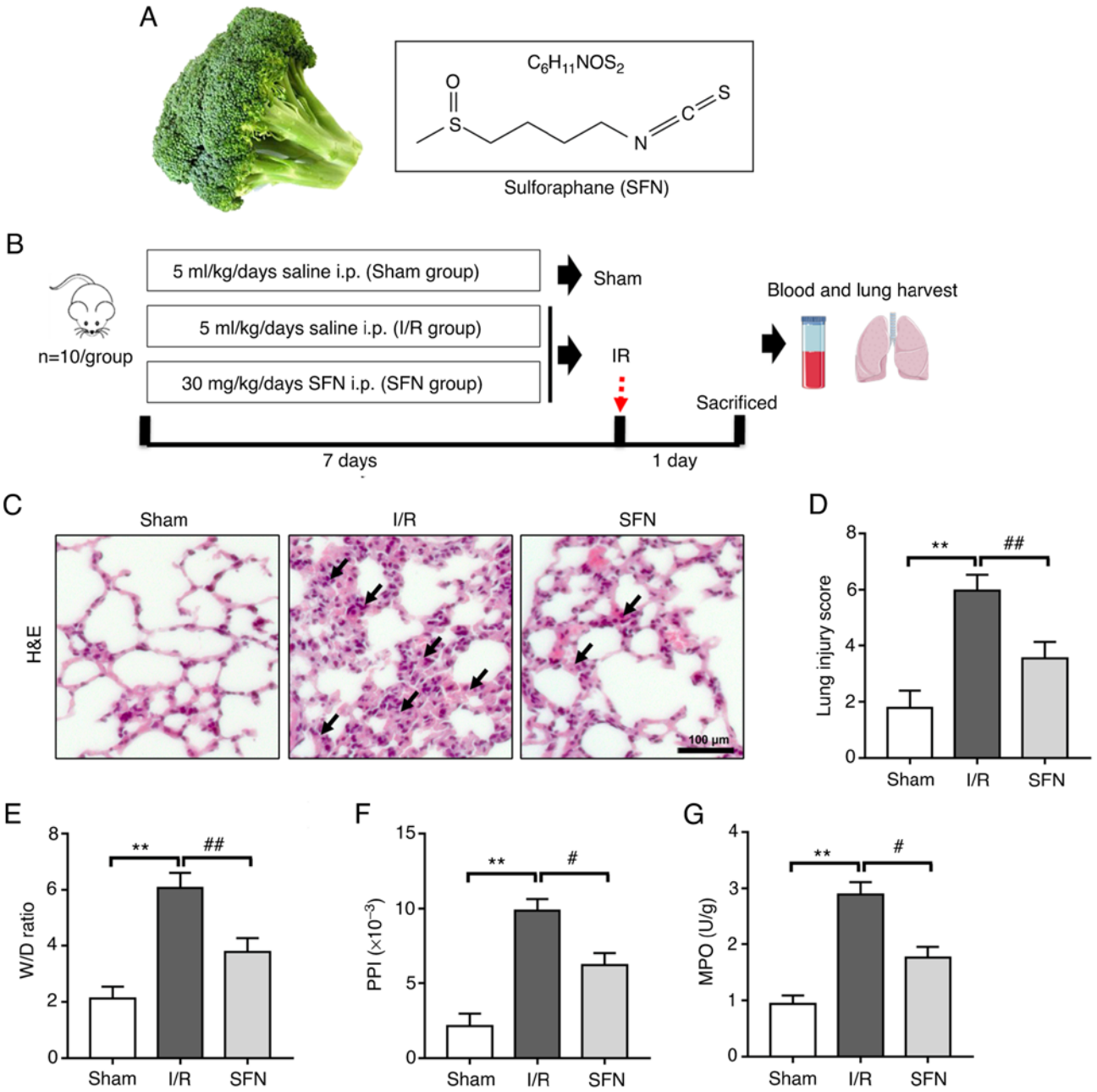

Figure 1. SFN attenuates I/R-induced lung lesions in rats. (A) Schematic representation of the chemical structure of the isothiocyanate sulforaphane. (B) Schematic of experimental design. (C) Representative images of H&E stained lung sections. Scaler bar, 100 μm. H&E staining showed that the infiltration of inflammatory cells was reduced and the alveolar wall thinned gradually in the lungs of the SFN group compared with those of the I/R group. (D) Quantification of lung injury scores. (E) The W/D ratio, (F) PPI, and (G) MPO values of the lungs. Data are presented as the mean ± SD. **P<0.01, Sham vs. I/R group; $^{\#}$P<0.05, $^{\#\#}$P<0.01, I/R vs. SFN group. SFN, sulforaphane; I/R, ischemia/reperfusion; H&E, hematoxylin and eosin; i.p. intraperitoneal; W/D, wet/dry; PPI, pulmonary permeability index; MPO, myeloperoxidase.

end of the incubation. Stop solution (50 μl) was added to each well to terminate the reaction. The color in the well changed from blue to yellow. Absorbance at 450 nm was recorded using a VersaMax ELISA Microplate Reader (Molecular Devices, LLC) within 15 min. after adding stop solution. A colorimetric method was used to detect malondialdehyde (MDA; cat. no. A003-1-2; Nanjing Jiancheng Bioengineering Institute) levels in the lung tissues as previously described (25).

Detection of serum cytokines. Blood samples were collected from the femora artery after reperfusion. The levels of IL-6, IL-1β, and TNF-α in serum were then analyzed using the Pro™ Mouse Cytokine Panel kit (#5827, Bio-Rad Laboratories, USA) according to the manufacturer's instructions.

Western blot analysis. Total protein was extracted from lung tissues. Briefly, 100 mg of lung tissues were homogenized in RIPA buffer for 10 min followed by centrifugation at 13,000 x g for 10 min at 4˚C. The protein concentration was detected using a Bradford Assay kit (cat. no. P0006; Beyotime Institute of Biotechnology). Western blot analyses were performed as described previously (26). Briefly, SDS-PAGE was performed by heating the samples for 8 min at 100˚C and loading 10 μg/lane of the proteins onto a 5-15% linear acrylamide

Table I. Arterial blood gases at the end of reperfusion.

Group	pH	PaO_2 (mmHg)	$PaCO_2$ (mmHg)
Sham	7.35±0.11	262.21±18.12	55.22±6.41
Ischemia-reperfusion	7.12±0.08[a]	167.35±21.21[a]	76.61±6.71[a]
SFN	7.22±0.09[b]	214.10±23.54[b]	62.24±7.43[b]

[a]P<0.05, Sham vs. I/R group; [b]P<0.05, I/R vs. SFN group. All data are presented as the mean ± SD. SFN, Sulforaphane; PaO_2, arterial partial pressure of oxygen; $PaCO_2$, arterial partial pressure of carbon dioxide.

gradient gel. Following transfer to PVDF membranes, the membranes were blocked in 5% BSA (cat. no. SW3015, Beijing Solarbio Science & Technology Co., Ltd.) dissolved in TBST (20%Tween-20) for 2 h at room temperature, and subsequently treated overnight at 4˚C with primary antibodies against the following proteins: Nrf2 (1:3,000; cat. no. #12721), HO-1 (1:3,000; cat. no. #43966), NQO1 (1:3,000; cat. no. #62262), CAT (1:3,000; cat. no. #12980), Histone H3 (1:3,000; cat. no. #4499), Bax (1:3,000; cat. no. #14796), Bcl-2 (1:3,000; cat. no. #498), Cleaved Caspase-3 (1:3,000; cat. no. #9664), and β-actin (1:5,000; cat. no. #4970). All primary antibodies were obtained from Cell Signaling Technology, Inc. The membranes were then incubated with a secondary antibody [1:5,000; anti-rabbit IgG (H+L), cat. no. #14708; Cell Signaling Technology, Inc.) for 2 h at room temperature, followed by TBST washes. Chemiluminescent detection was performed using an ECL kit and a ChemiDoc Touch imaging system (Bio-Rad Laboratories, Inc.). ImageJ (version 1.53; National Institutes of Health was used for densitometry analysis.

TUNEL assay. Apoptosis was determined using a TUNEL assay with a TUNEL test kit (cat. no. T2190, Beijing Solarbio Science & Technology Co., Ltd.) according to the manufacturer's instructions. The lung tissues were placed in 10% formalin at room temperature overnight for paraffin embedding and then were sectioned into 5 μm thick slices and processed for TUNEL. Next, tissues were dehydrated, incubated with 0.9% NaCl for 5 min, then rinsed with PBS for 5 min, fixed in 4% paraformaldehyde at room temperature for 15 min, then rinsed twice with PBS (5 min per wash). The sections were mixed with biotinylated nucleotides and terminal deoxynucleotidyl transferase and incubated at 37˚C for 60 min. Following PBS washes, the lung tissues were blocked with 0.3% hydrogen peroxide and incubated with HRP-conjugated streptavidin at room temperature for 30 min, then washed three times with PBS and stained with hematoxylin at room temperature for 3 min. A total of 5 fields of view were automatically selected by Image-Pro Plus version 5.1 (Media Cybernetics, Inc.). The percentage of apoptotic cells was calculated for each field of view. The mean was calculated to obtain the percentage of apoptotic cells and the results are expressed as the apoptotic index (AI), calculated as: AI (%) = (apoptotic nuclei count / total nucleus count) x100%.

Immunohistochemistry. The lung tissues were fixed in 10% formalin for 24 h at 4˚C. Sections of paraffin-embedded specimens were sectioned into 5 μm thick slices and prepared as above. The sections were then rinsed with PBS after being incubated in 3 percent H_2O_2 for 10 min. Following DAB chromogen incubation at room temperature for 5 min, the sections were counterstained with hematoxylin. Images were taken using a Nikon Eclipse 80i microscope (magnification, x400; Nikon Corporation).

Statistical analysis. Statistical analysis was performed using SPSS version 19.0 (IBM Corp.). Data are presented as the mean ± SD of three independent repeats. A one-way ANOVA followed by a Tukey's post hoc test or an unpaired Student's t-test were used for comparisons between groups. P<0.05 was considered to indicate a statistically significant difference.

Results

SFN attenuates I/R-induced lung lesions in rats. To determine the effects of SFN on lung injury after I/R, hematoxylin-eosin staining for lung histology was evaluated (Fig. 1C). Notably, a disordered alveolar structure was observed in the I/R group, with significant pulmonary interstitial edema, and a large number of inflammatory cells in the alveolar cavity. However, pretreatment with SFN significantly attenuated I/R-induced lung injury histopathologically. All of these changes were corroborated by the histological scoring. Pretreatment with SFN significantly decreased the lung injury score. (Fig. 1D).

An increase in lung permeability will promote the occurrence of pulmonary edema (27). Here, the extent of pulmonary edema based on the W/D ratio and PPI was assessed. As shown in Fig. 1E-F, the W/D ratio and PPI were markedly increased after I/R compared with the Sham group. SFN pretreatment significantly decreased the W/D ratio and PPI in the I/R rats. MPO activity was next assessed to evaluate neutrophil accumulation in the lung tissues. As shown in Fig. 1G, I/R treatment significantly increased MPO activity, whereas MPO activity was significantly reduced by SFN pretreatment.

Rat arterial blood gas analysis was performed to further assess lung injury. As shown in Table I, the arterial blood pH value was significantly decreased after I/R compared with the Sham group, and the I/R-induced acidosis was significantly prevented by SFN pretreatment. In addition, pretreatment with SFN also significantly prevented the increase in $PaCO_2$ and decrease in PaO_2 values in the I/R-induced rats. These results indicate that SFN pretreatment attenuated I/R-induced lung lesions in rats.

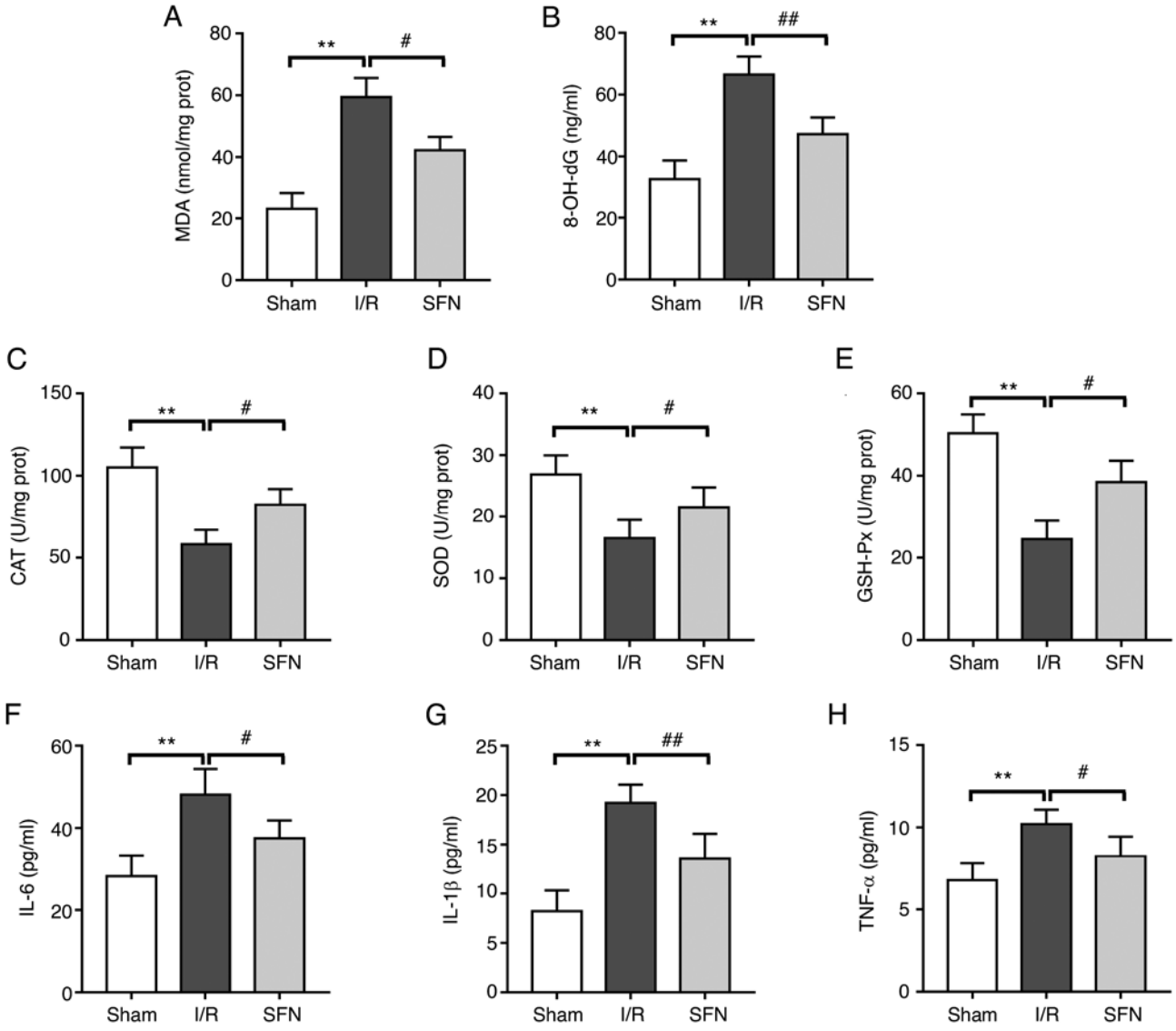

Figure 2. SFN alleviates I/R-induced lung oxidative stress and inflammation in rats. The levels of (A) MDA and (B) 8-OH-dG oxidative stress parameters. The antioxidant enzyme activities of (C) CAT, (D) SOD, and (E) GSH-Px. The levels of serum inflammatory cytokines (F) IL-6, (G) IL-1β, and (H) TNF-α. Data are presented as the mean ± SD. **P<0.01, Sham vs. I/R group; $^{\#}$P<0.05, $^{\#\#}$P<0.01, I/R vs. SFN group. SFN, sulforaphane; I/R, ischemia/reperfusion; MDA, malondialdehyde; CAT, catalase; SOD, superoxide dismutase; GSH-Px, glutathione peroxidase; prot, protein.

SFN alleviates I/R-induced oxidative stress and inflammation in the lungs of rats. The effect of SFN pretreatment on the redox metabolism and inflammatory response in the lungs of I/R rats was next evaluated. As shown in Fig. 2A and B, compared with the Sham group, the levels of MDA and 8-OH-dG were significantly increased in the I/R group. However, SFN pretreatment significantly downregulated the levels of MDA and 8-OH-dG in the I/R-induced rats. In addition, pretreatment with SFN markedly reversed the decrease in the antioxidant enzyme activities of CAT, SOD, and GSH-Px in the lung of I/R treated rats (Fig. 2C-E). Furthermore, serum IL-6, IL-1β, and TNF-α levels in the I/R group were significantly increased compared with those in the Sham group, and a significant decrease was observed in the SFN pretreatment group (Fig. 2F-H). These results show that SFN pretreatment alleviated the I/R-induced imbalance of redox metabolism and the aggravation of inflammatory reactions in the lungs of rats.

SFN improves I/R-induced lung apoptosis in rats. TUNEL staining was used to determine whether SFN attenuated lung tissue apoptosis following I/R in rats. As shown in Fig. 3A and B, the results of the TUNEL assays showed a significant increase in the AI in the I/R group compared with the Sham group, and SFN pretreatment significantly decreased the AI in the lung tissues of the I/R rats.

To determine the potential molecular mechanism of SFN in reducing lung apoptosis in I/R rats, the expression of several apoptosis-associated proteins in the lung tissues was measured (Fig. 3C). As shown in Fig. 3D-F, the expression of the pro-apoptotic proteins Bax and C-casp-3 were significantly increased, whereas the expression of the anti-apoptotic protein Bcl-2 was markedly decreased in the I/R group compared with the Sham group. SFN pretreatment notably attenuated the decrease in Bcl-2 expression and the increase in Bax and C-casp-3 expression compared with the I/R group. These data showed that SFN improved

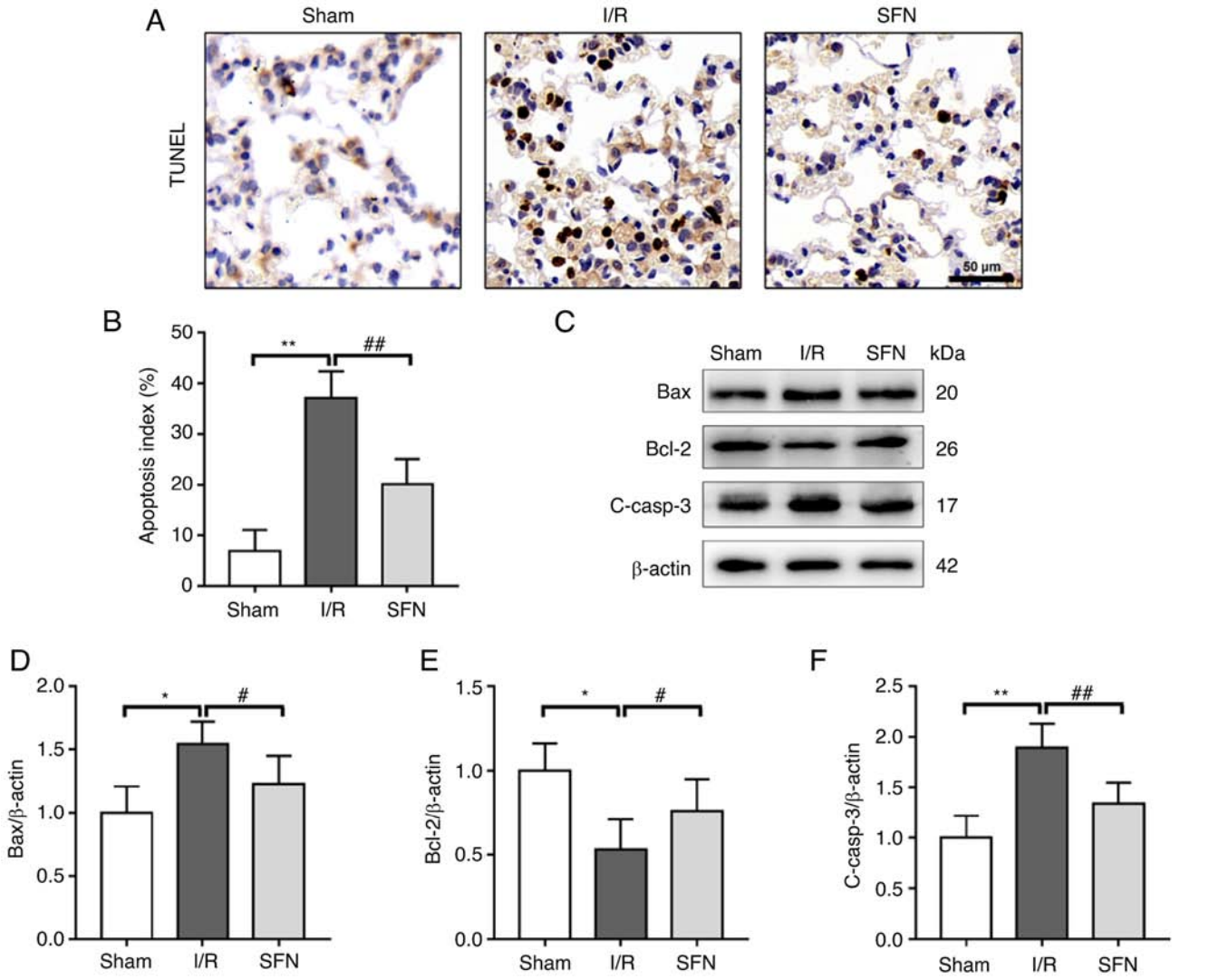

Figure 3. SFN improves I/R-induced lung apoptosis in rats. (A) Representative images of TUNEL-stained lung sections. (B) Quantification of the apoptosis index. (C) The protein expression levels of the Bax/Bcl-2 pathway members were evaluated by western blotting. Densitometry analysis of (D) Bcl-2, (E) Bax, and (F) C-casp3 protein expression levels. Data are presented as the mean ± SD. *P<0.05, **P<0.01, Sham vs. I/R group; $^{\#}$P<0.05, $^{\#\#}$P<0.01, I/R vs. SFN group. SFN group. SFN, sulforaphane; I/R, ischemia/reperfusion; C-casp3, cleaved-caspase 3.

I/R-induced lung apoptosis in rats by suppressing the Bax/Bcl-2 pathway.

SFN protects against I/R-induced lung lesions via activation of the Nrf2/HO-1 pathway. It has been shown that the Nrf2/HO-1 pathway plays an important role in maintaining redox metabolism and inhibiting apoptosis in lung tissues (28). Thus, the expression of Nrf2 and its downstream antioxidant genes in the lung tissues of I/R rats with or without SFN pretreatment was assessed (Fig. 4A). As shown in Fig. 4B, the nuclear transfer of Nrf2 (n-Nrf2) was markedly increased in the I/R group compared with the Sham group. Accordingly, the expression levels of Nrf2 target antioxidant genes HO-1, NQO1, and CAT were also markedly increased in the I/R group compared with the Sham group (Fig. 4C-E). Interestingly, SFN pretreatment further increased the expression of n-Nrf2 and its downstream antioxidant genes compared with the I/R group (Fig. 4B-E). These results suggested that SFN protected against I/R-induced lung lesions in rats via activation of the Nrf2/HO-1 pathway.

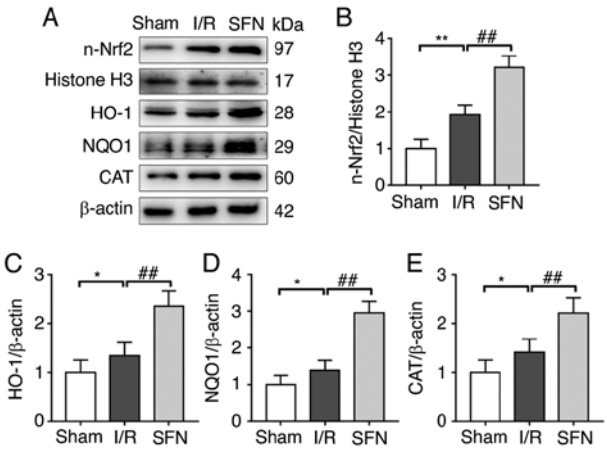

Figure 4. SFN protects against I/R-induced lung lesions via activation of the Nrf2/HO-1 pathway. (A) The protein expression levels of the Nrf2/HO-1 pathway members were evaluated by western blotting. Densitometry analysis of (B) nuclear Nrf2, (C) HO-1, (D) NQO1, and (E) CAT protein expression levels. Data are presented as the mean ± SD. *P<0.05, **P<0.01, Sham vs. I/R group; $^{\#\#}$P<0.01, I/R vs. SFN group. SFN group. SFN, sulforaphane; I/R, ischemia/reperfusion; CAT, catalase.

Discussion

As lung I/R injury is a recognized fatal complication following lung transplantation, there is an urgent need to identify novel therapeutic targets for alleviating lung I/R injury. I/R is directly related to the formation of ROS, increased vascular permeability, the activation of neutrophils, and cytokine release (29). The findings of the present study demonstrate that SFN can protect the lung against I/R-induced oxidative stress and inflammation, as evidenced by reducing ROS production and the release of pro-inflammatory cytokines. The beneficial effects of SFN on lung I/R injury involved activation of the Nrf2-related antioxidant pathway.

Oxidative stress is the outcome of an imbalance between the generation of ROS and the antioxidant defense systems, which is characterized by increases in ROS and other free radicals, leading to cellular injury (30). Oxidative stress is closely associated with the initiation and progression of lung I/R injury (31). The Nrf2-related pathway is considered a defense system aimed to counteract oxidative stress and preserve cellular homeostasis (32-34). Under physiological conditions, Nrf2 binds to its negative regulator Keap1 and is maintained in an inactive state. In the presence of ROS, Nrf2 dissociates from Keap1 and translocates to the nucleus, and binds to Maf (35,36). The Nrf2-Maf heterodimers then bind to antioxidant response elements in the promoters of key antioxidant genes (such as HO-1, NQO1, and CAT) and activates their transcription (37,38). HO-1 catalyzes the breakdown of heme to produce biliverdin, ferrous ions, and carbon monoxide, all of which are essential components of the inflammatory process (39). The homodimeric luteinase NQO1 promotes the elimination of hydrazine, which can produce harmful semihydroquinone radicals through the redox cycle, by catalyzing the reduction of hydrazine to hydroquinone (26,39). CAT promotes the synthesis of intracellular catalase, which catalyzes the decomposition of H_2O_2 into H_2O and O_2 (40). By scavenging excessive ROS levels and restoring redox homeostasis, Nrf2 can prevent I/R-related disorders (41). As previously described, SFN is a bioactive molecule present in broccoli, which exerts its cytoprotective effect by activating an Nrf2-related pathway (42). In this study, the expression of Nrf2 and its downstream target genes HO-1 and NQO1 were significantly decreased in the I/R rats, and SFN treatment significantly suppressed ROS generation and activated the Nrf2 antioxidant pathway, thus exerting therapeutic effects on IRI-induced injury by restoring cellular ROS homeostasis.

It is well established that the over-production of pro-inflammatory cytokines is another crucial trigger of cellular damage (43,44). Oxidative stress is closely correlated with the inflammatory response, especially during the I/R injury process. High levels of ROS produced during oxidative stress stimulate the release of pro-inflammatory mediators and increase inflammation, which may further aggravate I/R injury. In addition, activation of Nrf2 not only inhibits oxidative stress response but also contributes to the anti-inflammatory process by regulating cytokine secretion (45). SFN is a natural product that exerts its beneficial effects via the activation of the antioxidant systems and suppression of pro-inflammatory responses through the activation of Nrf2-related pathways (46,47). In the present study, elevated levels of pro-inflammatory cytokines were observed in the I/R rats, which were also effectively attenuated by SFN treatment. In line with the results of the present study, SFN was reported to ameliorate LPS-induced ROS, reactive nitrogen species, pro-inflammatory cytokine production, and cell death via Nrf2 activation (48).

Oxidative stress and inflammation are two major factors involved in the pathogenesis of lung I/R injury, which jointly contribute to the apoptosis of lung cells. Apoptosis is closely associated with the pathological process of lung I/R injury, according to earlier studies (49,50). Bcl-2, an anti-apoptotic protein, can inhibit the production of free radicals and endoplasmic reticulum Ca^{2+} as well as prevent the formation of lipid peroxides (51). Bax is an endogenous antagonist of Bcl-2; by physically attaching to the related protein homologs, it inhibits Bcl-2, thus inducing apoptosis (52). Bcl-2 and Bax expression levels are typically balanced in a healthy state (53). In the present study, it was found that lung cell apoptosis was activated in rats with I/R lung injury and that Bax protein expression increased while Bcl-2 protein expression was decreased. An important biochemical aspect of apoptosis is the activation of caspases. The beginning and completion of mammalian apoptotic processes are regulated by the caspase family of cysteine proteases (54). Caspase-3 is created from a 32 kDa zymogen and cleaves to a 17 kDa active subunit via mitochondrial and death ligand mechanisms (55). This zymogen is a crucial caspase effector that starts the cell's disintegration during the final stages of apoptosis (56). In the present study, it was found that SFN effectively inhibited the expression level of the pro-apoptotic proteins Bax and C-casp-3 in the I/R group rats, thus reducing apoptosis. A previous study showed that Nrf2/HO-1 activation counteracts the inflammatory response and apoptosis in contrast-induced renal injury (57). Herein, the beneficial effects of SFN on I/R injury via antioxidative stress, anti-inflammation, and anti-apoptosis were dependent on the activation of the Nrf2/HO-1 pathway. Conversely, as mitochondria are the primary source of ROS, the destruction of mitochondria leads to the accumulation of excessive ROS levels, resulting in increased mitochondrial dysfunction (58). MDA, SOD, and GSH are important indicators for detecting oxidative stress. Through a number of signaling mechanisms, the generation of ROS can lead to oxidative stress in cells and cause cells to undergo apoptosis (34,59). When mitochondria undergo apoptosis, the expression of Bcl-2 is inhibited (60). However, at present, whether SFN alleviates I/R-induced oxidative stress in lung tissue by alleviating mitochondrial damage remains to be further studied.

In summary, the present study provided evidence that SFN protected against lung I/R injury-induced oxidative injury, inflammation, and apoptosis via activation of the Nrf2/HO-1 pathway. These findings may provide novel insights into the development of therapeutic applications of SFN for lung I/R injury.

Acknowledgements

Not applicable.

Funding

No funding was received.

Availability of data and materials

The datasets used and/or analyzed during the current study are available from the corresponding author on reasonable request.

Authors' contributions

LZ and CY conceived and designed the experiments. SW and YZ performed the experiments. FL analyzed the data. LZ wrote the manuscript. All authors read and approved the final manuscript. LZ and CY confirm the authenticity of all the raw data.

Ethics approval and consent to participate

The present study was approved by the Ethics Committee of Yantai Mountain Hospital, Yantai, China (approval no. 2021-12.).

Patient consent for publication

Not applicable.

Competing interests

The authors declare that they have no competing interests.

References

1. Wei L, Li J, Han Z, Chen Z and Zhang Q: Silencing of lncRNA MALAT1 prevents inflammatory Injury after lung transplant ischemia-reperfusion by downregulation of IL-8 via p300. Mol Ther Nucleic Acids 18: 285-297, 2019.
2. Eltzschig HK and Eckle T: Ischemia and reperfusion-from mechanism to translation. Nat Med 17: 1391-1401, 2011.
3. Chen-Yoshikawa TF: Ischemia-reperfusion injury in lung transplantation. Cells 10: 1333, 2021.
4. Qin J, Su X, Jin X and Zhao J: Parecoxib mitigates lung ischemia-reperfusion injury in rats by reducing oxidative stress and inflammation and up-regulating HO-1 expression. Acta Cir Bras 36: e360901, 2021.
5. Guo Y, Liu Y, Zhao S, Xu W, Li Y, Zhao P, Wang D, Cheng H, Ke Y and Zhang X: Oxidative stress-induced FABP5 S-glutathionylation protects against acute lung injury by suppressing inflammation in macrophages. Nat Commun 12: 7094, 2021.
6. Kong L, Deng J, Zhou X, Cai B, Zhang B, Chen X, Chen Z and Wang W: Sitagliptin activates the p62-Keap1-Nrf2 signalling pathway to alleviate oxidative stress and excessive autophagy in severe acute pancreatitis-related acute lung injury. Cell Death Dis 12: 928, 2021.
7. Liao WI, Wu SY, Tsai SH, Pao HP, Huang KL and Chu SJ: 2-Methoxyestradiol protects against lung ischemia/reperfusion injury by upregulating annexin A1 protein expression. Front Immunol 12: 596376, 2021.
8. Vanduchova A, Anzenbacher P and Anzenbacherova E: Isothiocyanate from Broccoli, Sulforaphane, and its properties. J Med Food 22: 121-126, 2019.
9. Russo M, Spagnuolo C, Russo GL, Skalicka-Woźniak K, Daglia M, Sobarzo-Sánchez E, Nabavi SF and Nabavi SM: Nrf2 targeting by sulforaphane: A potential therapy for cancer treatment. Crit Rev Food Sci Nutr 58: 1391-1405, 2018.
10. Dana AH and Alejandro SP: Role of sulforaphane in endoplasmic reticulum homeostasis through regulation of the antioxidant response. Life Sci 299: 120554, 2022.
11. Bajpai VK, Alam MB, Quan KT, Kwon KR, Ju MK, Choi HJ, Lee JS, Yoon JI, Majumder R, Rather IA, *et al*: Antioxidant efficacy and the upregulation of Nrf2-mediated HO-1 expression by (+)-lariciresinol, a lignan isolated from Rubia philippinensis, through the activation of p38. Sci Rep 7: 46035, 2017.
12. Franke M, Bieber M, Kraft P, Weber ANR, Stoll G and Schuhmann MK: The NLRP3 inflammasome drives inflammation in ischemia/reperfusion injury after transient middle cerebral artery occlusion in mice. Brain Behav Immun 92: 223-233, 2021.
13. Zhao HD, Zhang F, Shen G, Li YB, Li YH, Jing HR, Ma LF, Yao JH and Tian XF: Sulforaphane protects liver injury induced by intestinal ischemia reperfusion through Nrf2-ARE pathway. World J Gastroenterol 16: 3002-3010, 2010.
14. Peng N, Jin L, He A, Deng C and Wang X: Effect of sulphoraphane on newborn mouse cardiomyocytes undergoing ischaemia/reperfusion injury. Pharm Biol 57: 753-759, 2019.
15. Li D, Shao R, Wang N, Zhou N, Du K, Shi J, Wang Y, Zhao Z, Ye X, Zhang X and Xu H: Sulforaphane activates a lysosome-dependent transcriptional program to mitigate oxidative stress. Autophagy 17: 872-887, 2021.
16. Yan J, Li J, Zhang L, Sun Y, Jiang J, Huang Y, Xu H, Jiang H and Hu R: Nrf2 protects against acute lung injury and inflammation by modulating TLR4 and Akt signaling. Free Radic Biol Med 121: 78-85, 2018.
17. Han YK, Kim JS, Jang G and Park KM: Cisplatin induces lung cell cilia disruption and lung damage via oxidative stress. Free Radic Biol Med 177: 270-277, 2021.
18. Ishida K, Kaji K, Sato S, Ogawa H, Takagi H, Takaya H, Kawaratani H, Moriya K, Namisaki T, Akahane T and Yoshiji H: Sulforaphane ameliorates ethanol plus carbon tetrachloride-induced liver fibrosis in mice through the Nrf2-mediated antioxidant response and acetaldehyde metabolization with inhibition of the LPS/TLR4 signaling pathway. J Nutr Biochem 89: 108573, 2021.
19. Ding Y, Tu P, Chen Y, Huang Y, Pan X and Chen W: CYP2J2 and EETs protect against pulmonary arterial hypertension with lung ischemia-reperfusion injury in vivo and in vitro. Respir Res 22: 291, 2021.
20. Zhou A, Hong Y and Lv Y: Sulforaphane attenuates endometriosis in rat models through inhibiting PI3K/Akt signaling pathway. Dose Response 17: 1559325819855538, 2019.
21. Li D, Song LL, Wang J, Meng C and Cui XG: Adiponectin protects against lung ischemia-reperfusion injury in rats with type 2 diabetes mellitus. Mol Med Rep 17: 7191-7201, 2018.
22. Li X, Jamal M, Guo P, Jin Z, Zheng F, Song X, Zhan J and Wu H: Irisin alleviates pulmonary epithelial barrier dysfunction in sepsis-induced acute lung injury via activation of AMPK/SIRT1 pathways. Biomed Pharmacother 118: 109363, 2019.
23. Ma D, Gao W, Liu J, Kong D, Zhang Y and Qian M: Mechanism of oxidative stress and Keap-1/Nrf2 signaling pathway in bronchopulmonary dysplasia. Medicine (Baltimore) 99: e20433, 2020.
24. Zhou Y, Zhang L, Guan J and Yin X: Improvement of lung ischemia-reperfusion injury by inhibition of microRNA-155 via reductions in neuroinflammation and oxidative stress of vagal afferent nerve. Pulm Circ 10: 2045894020922125, 2020.
25. Dong H, Qiang Z, Chai D, Peng J, Xia Y, Hu R and Jiang H: Nrf2 inhibits ferroptosis and protects against acute lung injury due to intestinal ischemia reperfusion via regulating SLC7A11 and HO-1. Aging (Albany NY) 12: 12943-12959, 2020.
26. Wang Y, Han K, Li Z, Tang X, Wang C, Zhao Y, Zhang H, Geng Z, Kong J, Luan X and Xiong Y: Protective effect of hydroxysafflor yellow A on renal ischemia-reperfusion injury by targeting the Akt-Nrf2 axis in mice. Exp Ther Med 24: 741, 2022.
27. Chepurnova DA, Samoilova EV, Verin AD, Fesenko AG, Anisimov AA and Korotaeva AA: Inhibition of Meprins Reduces Pulmonary Edema in LPS-Induced Acute Lung Damage. Bull Exp Biol Med 166: 719-721, 2019.
28. Huang CY, Deng JS, Huang WC, Jiang WP and Huang GJ: Attenuation of lipopolysaccharide-Induced acute lung injury by hispolon in mice, Through Regulating the TLR4/PI3K/Akt/mTOR and Keap1/Nrf2/HO-1 pathways, and suppressing oxidative stress-mediated ER stress-induced apoptosis and autophagy. Nutrients 12: 1742, 2020.
29. Liu YY, Chiang CH, Hung SC, Chian CF, Tsai CL, Chen WC and Zhang H: Hypoxia-preconditioned mesenchymal stem cells ameliorate ischemia/reperfusion-induced lung injury. PLoS One 12: e0187637, 2017.
30. Liu Q, Gao Y and Ci X: Role of Nrf2 and Its activators in respiratory diseases. Oxid Med Cell Longev 2019: 7090534, 2019.
31. Ferrari RS and Andrade CF: Oxidative stress and lung ischemia-reperfusion injury. Oxid Med Cell Longev 2015: 590987, 2015.

32. Bellezza I, Giambanco I, Minelli A and Donato R: Nrf2-Keap1 signaling in oxidative and reductive stress. Biochim Biophys Acta Mol Cell Res 1865: 721-733, 2018.
33. Han B, Li S, Lv Y, Yang D, Li J, Yang Q, Wu P, Lv Zand Zhang Z: Dietary melatonin attenuates chromium-induced lung injury via activating the Sirt1/Pgc-1α/Nrf2 pathway. Food Funct 10: 5555-5565, 2019.
34. Zhang H, Tan X, Yang D, Lu J, Liu B, Baiyun R and Zhang Z: Dietary luteolin attenuates chronic liver injury induced by mercuric chloride via the Nrf2/NF-κB/P53 signaling pathway in rats. Oncotarget 8: 40982-40993, 2017.
35. Nguyen T, Nioi P and Pickett CB: The Nrf2-antioxidant response element signaling pathway and its activation by oxidative stress. J Biol Chem 284: 13291-13295, 2009.
36. Yang D, Lv Z, Zhang H, Liu B, Jiang H, Tan X, Lu J, Baiyun R and Zhang Z: Activation of the Nrf2 signaling pathway involving KLF9 plays a critical role in allicin resisting against arsenic trioxide-induced hepatotoxicity in rats. Biol Trace Elem Res 176: 192-200, 2017.
37. Shaw P and Chattopadhyay A: Nrf2-ARE signaling in cellular protection: Mechanism of action and the regulatory mechanisms. J Cell Physiol 235: 3119-3130, 2020.
38. Baird L, Swift S, Lleres D and Dinkova-Kostova AT: Monitoring Keap1-Nrf2 interactions in single live cells. Biotechnol Adv 32: 1133-1144, 2014.
39. Xiang Q, Zhao Y, Lin J, Jiang S and Li W: The Nrf2 antioxidant defense system in intervertebral disc degeneration: Molecular insights. Exp Mol Med 54: 1067-1075, 2022.
40. Xiong Y, Xiong Y, Zhang H, Zhao Y, Han K, Zhang J, Zhao D, Yu Z, Geng Z, Wang L, *et al*: hPMSCs-derived exosomal miRNA-21 protects against aging-related oxidative damage of CD4(+) T cells by targeting the PTEN/PI3K-Nrf2 axis. Front Immunol 12: 780897, 2021.
41. Cadenas S: ROS and redox signaling in myocardial ischemia-reperfusion injury and cardioprotection. Free Radic Biol Med 117: 76-89, 2018.
42. Liebman SE and Le TH: Eat Your Broccoli: Oxidative stress, NRF2, and sulforaphane in chronic kidney disease. Nutrients 13: 266, 2021.
43. Dolivo D, Rodrigues A, Sun L, Galiano R, Mustoe T and Hong SJ: Reduced hydration regulates pro-inflammatory cytokines via CD14 in barrier function-impaired skin. Biochim Biophys Acta Mol Basis Dis 1868: 166482, 2022.
44. Ijaz S, Mohammed I, Gholaminejhad M, Mokhtari T, Akbari M and Hassanzadeh G: Modulating pro-inflammatory cytokines, tissue damage magnitude, and motor deficit in spinal cord injury with subventricular zone-derived extracellular vesicles. J Mol Neurosci 70: 458-466, 2020.
45. Ahmed SM, Luo L, Namani A, Wang XJ and Tang X: Nrf2 signaling pathway: Pivotal roles in inflammation. Biochim Biophys Acta Mol Basis Dis 1863: 585-597, 2017.
46. Juge N, Mithen RF and Traka M: Molecular basis for chemoprevention by sulforaphane: A comprehensive review. Cell Mol Life Sci 64: 1105-1127, 2007.
47. Ruhee RT and Suzuki K: The integrative role of sulforaphane in preventing inflammation, oxidative stress and fatigue: A review of a potential protective phytochemical. Antioxidants (Basel) 9: 521, 2020.
48. Eren E, Tufekci KU, Isci KB, Tastan B, Genc K and Genc S: Sulforaphane Inhibits lipopolysaccharide-induced inflammation, cytotoxicity, oxidative stress, and miR-155 expression and switches to mox phenotype through activating extracellular signal-regulated kinase 1/2-nuclear factor erythroid 2-related factor 2/antioxidant response element pathway in murine microglial cells. Front Immunol 9: 36, 2018.
49. Sancho-Martinez SM, Lopez-Novoa JM and Lopez-Hernandez FJ: Pathophysiological role of different tubular epithelial cell death modes in acute kidney injury. Clin Kidney J 8: 548-559, 2015.
50. Li Y, Cao Y, Xiao J, Shang J, Tan Q, Ping F, Huang W, Wu F, Zhang H and Zhang X: Inhibitor of apoptosis-stimulating protein of p53 inhibits ferroptosis and alleviates intestinal ischemia/reperfusion-induced acute lung injury. Cell Death Differ 27: 2635-2650, 2020.
51. Saitoh Y, Ouchida R, Kayasuga A and Miwa N: Anti-apoptotic defense of bcl-2 gene against hydroperoxide-induced cytotoxicity together with suppressed lipid peroxidation, enhanced ascorbate uptake, and upregulated Bcl-2 protein. J Cell Biochem 89: 321-334, 2003.
52. Renault TT and Chipuk JE: Death upon a kiss: Mitochondrial outer membrane composition and organelle communication govern sensitivity to BAK/BAX-dependent apoptosis. Chem Biol 21: 114-123, 2014.
53. Ye Q, Zhu YI, Ye S, Liu H, She X, Niu Y and Ming Y: Gypenoside attenuates renal ischemia/reperfusion injury in mice by inhibition of ERK signaling. Exp Ther Med 11: 1499-1505, 2016.
54. Hu L, Chen L, Yang G, Li L, Sun H, Chang Y, Tu Q, Wu M and Wang H: HBx sensitizes cells to oxidative stress-induced apoptosis by accelerating the loss of Mcl-1 protein via caspase-3 cascade. Mol Cancer 10: 43, 2011.
55. Yang D, Han B, Baiyun R, Lv Z, Wang X, Li S, Lv Y, Xue J, Liu Y and Zhang Z: Sulforaphane attenuates hexavalent chromium-induced cardiotoxicity via the activation of the Sesn2/AMPK/Nrf2 signaling pathway. Metallomics 12: 2009-2020, 2020.
56. Yang X, Fang Y, Hou J, Wang X, Li J, Li S, Zheng X, Liu Y and Zhang Z: The heart as a target for deltamethrin toxicity: Inhibition of Nrf2/HO-1 pathway induces oxidative stress and results in inflammation and apoptosis. Chemosphere 300: 134479, 2022.
57. Gao Z, Han Y, Hu Y, Wu X, Wang Y, Zhang X, Fu J, Zou X, Zhang J, Chen X, *et al*: Targeting HO-1 by epigallocatechin-3-gallate reduces contrast-induced renal injury via Anti-oxidative stress and anti-inflammation pathways. PLoS One 11: e0149032, 2016.
58. Patel J, Baptiste BA, Kim E, Hussain M, Croteau DL and Bohr VA: DNA damage and mitochondria in cancer and aging. Carcinogenesis 41: 1625-1634, 2020.
59. Han B, Lv Z, Han X, Li S, Han B, Yang Q, Wang X, Wu P, Li J, Deng N and Zhang Z: Harmful effects of inorganic mercury exposure on kidney cells: Mitochondrial dynamics disorder and excessive oxidative stress. Biol Trace Elem Res 200: 1591-1597, 2022.
60. Zhang L, Huang X, Guo T, Wang H, Fan H and Fang L: Study of cinobufagin as a promising anticancer agent in uveal melanoma through intrinsic apoptosis pathway. Front Oncol 10: 325, 2020.